GEOLOGY | THE GEOLOGICAL SOCIETY OF AMERICA®

https://doi.org/10.1130/G47781.1

Manuscript received 20 April 2020
Revised manuscript received 29 June 2020
Manuscript accepted 6 July 2020

Ocean acidification during the early Toarcian extinction event: Evidence from boron isotopes in brachiopods

Tamás Müller[1,*], Hana Jurikova[2,3], Marcus Gutjahr[2], Adam Tomašových[1], Jan Schlögl[4], Volker Liebetrau[2], Luís v. Duarte[5], Rastislav Milovský[1], Guillaume Suan[6], Emanuela Mattioli[6,7], Bernard Pittet[6] and Anton Eisenhauer[2]

[1]Earth Science Institute, Slovak Academy of Sciences, Ďumbierska 1, 974 01 Banská Bystrica, Slovakia
[2]GEOMAR Helmholtz-Zentrum für Ozeanforschung Kiel, Wischhofstr. 1-3, 24148 Kiel, Germany
[3]GFZ Deutsches GeoForschungsZentrum–Helmholtz-Zentrum Potsdam, Telegrafenberg, 14473 Potsdam, Germany
[4]Department of Geology and Paleontology, Faculty of Natural Sciences, Comenius University in Bratislava, Mlynská dolina, Ilkovičova 6, SK-842 15 Bratislava, Slovakia
[5]University of Coimbra, MARE–Marine and Environmental Sciences Centre–Department of Earth Sciences, Polo II, Rua Sílvio Lima, 3030-790 Coimbra, Portugal
[6]Univ Lyon, Univ Lyon 1, ENSL, CNRS, LGL-TPE, F-69622, Villeurbanne, France
[7]Institut Universitaire de France (IUF), 75231 Paris Cedex 05, France

ABSTRACT

The loss of carbonate production during the Toarcian Oceanic Anoxic Event (T-OAE, ca. 183 Ma) is hypothesized to have been at least partly triggered by ocean acidification linked to magmatism from the Karoo-Ferrar large igneous province (southern Africa and Antarctica). However, the dynamics of acidification have never been directly quantified across the T-OAE. Here, we present the first record of temporal evolution of seawater pH spanning the late Pliensbachian and early Toarcian from the Lusitanian Basin (Portugal) reconstructed on the basis of boron isotopic composition ($\delta^{11}B$) of brachiopod shells. $\delta^{11}B$ declines by ~1‰ across the Pliensbachian-Toarcian boundary (Pl-To) and attains the lowest values (~12.5‰) just prior to and within the T-OAE, followed by fluctuations and a moderately increasing trend afterwards. The decline in $\delta^{11}B$ coincides with decreasing bulk $CaCO_3$ content, in parallel with the two-phase decline in carbonate production observed at global scales and with changes in pCO_2 derived from stomatal indices. Seawater pH had declined significantly already prior to the T-OAE, probably due to the repeated emissions of volcanogenic CO_2. During the earliest phase of the T-OAE, pH increased for a short period, likely due to intensified continental weathering and organic carbon burial, resulting in atmospheric CO_2 drawdown. Subsequently, pH dropped again, reaching the minimum in the middle of the T-OAE. The early Toarcian marine extinction and carbonate collapse were thus driven, in part, by ocean acidification, similar to other Phanerozoic events caused by major CO_2 emissions and warming.

INTRODUCTION

The Pliensbachian-Toarcian (Pl-To) boundary and the Toarcian Oceanic Anoxic Event (T-OAE, ca. 183 Ma) constituted a transient interval of global warming, development of widespread anoxia, enhanced organic carbon burial, and acceleration of the hydrological cycle, resulting in a mass extinction and a collapse of carbonate production (e.g., Jenkyns, 1988; Bailey et al., 2003; Cohen et al., 2004; Suan et al., 2010; Trecalli et al., 2012). These changes and the associated ecosystem crisis have been linked to the emplacement of the Karoo-Ferrar large igneous province (southern Africa and Antarctica) and consequent greenhouse gas release (Caruthers et al., 2013). During the T-OAE, volcanogenic greenhouse gas emissions induced by thermal metamorphosis of coal deposits in the Karoo basin most likely triggered carbon-cycle perturbations (McElwain et al., 2005; Percival et al., 2015), although other sources, such as dissociation of methane hydrates from marine sediments or terrestrial methane, have also been postulated (Hesselbo et al., 2000; Them et al., 2017).

The changes in the carbon cycle are globally expressed as a short negative shift in the carbon-isotope record at the Pl-To boundary (Littler et al., 2010), followed by a broad positive excursion that is interrupted by a major negative (~6‰) carbon isotope excursion (CIE) during the T-OAE (Hesselbo et al., 2007; Müller et al., 2017). Marine carbonate factories dominated by bivalves, corals, and algae disappeared after the onset of the negative CIE (Trecalli et al., 2012; Brame et al., 2019), and nannoplankton fluxes declined in epicontinental basins (Mattioli et al., 2009). The coincidence between the timing of the CIE, indicating a major increase in CO_2 emissions, and the collapse in carbonate production indicate ocean acidification as one of the potential drivers of these changes (Trecalli et al., 2012). However, a direct quantification of pH is lacking. To fill this gap, we measured the boron isotope composition ($\delta^{11}B$) of brachiopod shells in conjunction with their $\delta^{13}C$ and $\delta^{18}O$ from the Peniche section (Global Boundary Stratotype Section and Point of the Toarcian Stage) in the Lusitanian Basin (Portugal; Comas-Rengifo et al., 2015; Duarte, 2007). This section combines exceptional stratigraphic resolution across the Pl-To boundary and the T-OAE with reliable preservation of geochemical signals in calcitic shells (Suan et al., 2008; Rocha et al., 2016). Here, we evaluate the timing and intensity of ocean acidification by reconstructing temporal evolution of seawater pH.

*E-mail: beregond02@gmail.com

CITATION: Müller, T., et al., 2020, Ocean acidification during the early Toarcian extinction event: Evidence from boron isotopes in brachiopods: Geology, v. 48, p. , https://doi.org/10.1130/G47781.1

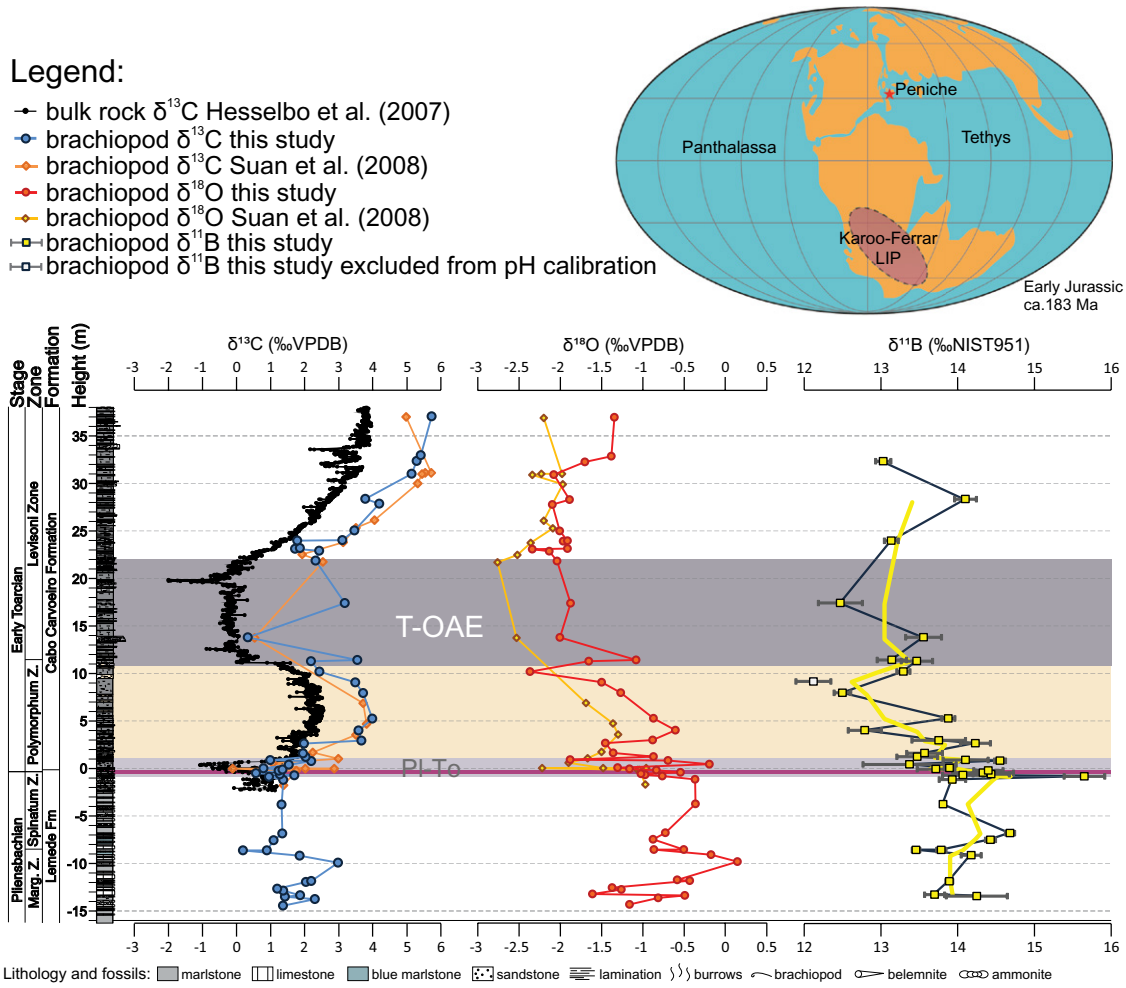

Figure 1. (Upper panel) Paleogeographic location of the Lusitanian Basin (Portugal; red star) during the Early Jurassic (adapted from Ikeda and Hori, 2014). LIP—large igneous province. (Lower panel) Stratigraphic log and scale (after Hesselbo et al., 2007; modified following Duarte et al., 2018) plotted against bulk $\delta^{13}C$ (Hesselbo et al., 2007) and published (Suan et al., 2008) and new (this study) brachiopod $\delta^{13}C$, $\delta^{18}O$, and $\delta^{11}B$ (error bars indicate two standard deviations on replicated analyses). Yellow line shows the three-point moving average; horizontal purple line indicates the exact level of the Pliensbachian-Toarcian boundary. The Toarcian Oceanic Anoxic Event (T-OAE) is defined as the interval between onset of negative carbon isotope excursion and the inflection point in the Levisoni ammonite zone, above which values tend toward a more positive direction, and coincides with the deposition of organic-rich black shales in many European sections (Müller et al., 2017). Pl-To—Pliensbachian-Toarcian boundary; Z.—Zone; Marg.—Margaritatus; Fm.—Formation; VPDB—Vienna Peedee belemnite; NIST951—Boric acid isotopic standard.

METHODS

The $\delta^{11}B$ composition of marine biogenic carbonates is presently regarded as the most reliable pH proxy (Gutjahr et al., 2017). Articulate brachiopods secrete low-Mg calcitic shells nearly in isotopic equilibrium with seawater (Brand et al., 2013) and exhibit a pH-dependent $\delta^{11}B$ relationship (Lécuyer et al., 2002; Penman et al., 2013; Jurikova et al., 2019). We present major- and trace-element concentration, $\delta^{11}B$, $\delta^{13}C$, and $\delta^{18}O$, as well as $^{87}Sr/^{86}Sr$ composition of brachiopod shells collected from the upper Pliensbachian and lower Toarcian at the Peniche section, covering 51.5 m of the section (Fig. 1) and spanning ~3.8 m.y. (see the Supplemental Material[1]). Sample preparation and elemental, as well as $\delta^{11}B$ and $^{87}Sr/^{86}Sr$, analyses were performed according to the methods of Jurikova et al. (2019) and Krabbenhöft et al. (2009) on pre-cleaned dissolved powders, with major- and trace-element content (Ca, Mg, Al, Sr, Mn, B) determined on a quadrupole inductively coupled plasma–mass spectrometer (ICP-MS) (Agilent 7500x), $\delta^{11}B$ on a multicollector ICP-MS (Thermo Scientific Neptune Plus), and $^{87}Sr/^{86}Sr$ via thermal ionization mass spectrometry (TIMS) (ThermoFisher TRITON). $\delta^{13}C$ and $\delta^{18}O$ were measured using a MAT253 isotope-ratio mass spectrometer coupled with a Kiel IV (ThermoFisher Scientific) carbonate device (see the Supplemental Material and Table S1 therein).

To quantify pH from $\delta^{11}B$ values, we first tied our initial $\delta^{11}B$-derived seawater pH from late Pliensbachian brachiopods to pre-event conditions (pH = 7.7) based on a Phanerozoic pH model for a Neritan ocean (Ridgwell, 2005) because carbonate production was predominantly neritic during the Early Jurassic. The pH in this model has a mean value of 7.7 and ranges between 7.4 and 7.9 for the latest Pliensbachian (ca. 184 Ma). With this range of pre-event seawater pH, we computed $\delta^{11}B_{seawater}$ and seawater pH with two different $\delta^{11}B$-pH calibrations: (1) scenario 1, where biological influence on boron incorporation into brachiopod shells is considered (Lécuyer et al., 2002), resulting in a mean $\delta^{11}B_{seawater}$ of 36.6‰ (range = 34.9‰–37.5‰); and (2) scenario 2, where boron incorporation follows inorganic fractionation ($\delta^{11}B_{brachiopod} = \delta^{11}B_{borate}$; based on Klochko et al. [2006]), resulting in a mean $\delta^{11}B_{seawater}$ of 38.9‰ (range = 37‰–40‰) (Fig. 2; Fig. S2). Because brachiopods exert vital control over the incorporation of boron into their shells to some degree, we refer to scenario 1 below, while scenario 2 is discussed in the Supplemental Material. Using our $\delta^{11}B$-pH values and $\delta^{18}O$-based temperatures estimated on the basis of our brachiopod shells and the formerly published pCO_2 estimates from stomatal indices (McElwain et al., 2005; Steinthorsdottir and Vajda, 2015), we first calculated seawater alkalinity at ammonite subzone-scale

[1]Supplemental Material. Detailed information on the applied geochemical and calibration methods, carbonate chemistry models, age model, sample preservation, and additional information about species-specific effect on $\delta^{11}B$ fractionation in brachiopods. Please visit https://doi.org/10.1130/GEOL.S.12730832 to access the supplemental material, and contact editing@geosociety.org with any questions.

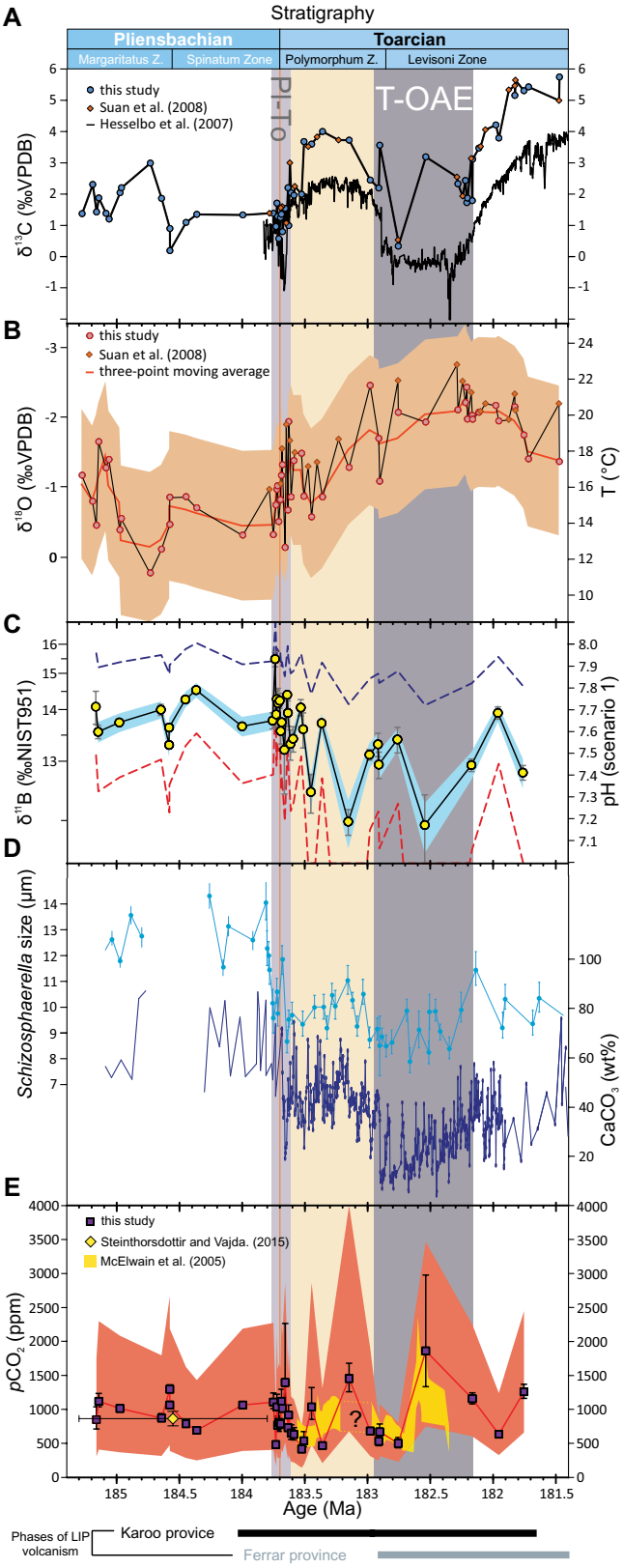

Figure 2. Multiproxy record across the Pliensbachian-Toarcian boundary (ammonite zone scale resolution). Pl-To—Pliensbachian-Toarcian boundary; T-OAE—Toarcian Oceanic Anoxic Event; Z.—Zone. (A) Bulk-rock carbon isotope data (Hesselbo et al., 2007) and brachiopod carbon isotope data (this study; Suan et al., 2008). VPDB—Vienna Peedee belemnite. (B) Brachiopod oxygen isotope and calibrated temperature record (this study; Suan et al., 2008); orange band is error envelope for temperature estimation, assuming seawater $\delta^{18}O$ of –2‰ to 0‰ (equivalent to salinity ±2.5 ppt). (C) Boron isotope and calibrated pH record according to scenario 1 described in text (yellow symbols; Lécuyer et al., 2002); blue band shows propagated uncertainty based on analytical uncertainty for $\delta^{11}B$ (±0.2‰, two standard deviations). Dashed lines mark limits of pH envelope derived from minimum and maximum pH of late Pliensbachian pH Neritan model of Ridgwell (2005). Plot is truncated at pH value 7 due to fact that some values fell below effective range of pH calibrations. NIST951—Boric acid isotopic standard. (D) Size of calcareous nannofossil *Schizosphaerella* (light blue) and bulk rock $CaCO_3$ content (dark blue) (Suan et al., 2010). Error bars: ± 1 standard error of *Schizosphaerella* major axis size. (E) pCO_2 records (previous and new) with uncertainties (orange area; see the Supplemental Material [see footnote 1]). Ages for the Karoo-Ferrar large igneous province (LIP) are after Ruebsam et al. (2019). See the Supplemental Material for further details on our age model.

stratigraphic resolution using the R package *seacarb* (https://cran.r-project.org/web/packages/seacarb/seacarb.pdf; Gattuso 2019) (Fig. S4). Second, we recomputed the atmospheric pCO_2 record on the basis of alkalinity (with constant values for each subzone), $\delta^{11}B$ pH, and $\delta^{18}O$-based temperature values at bed-scale resolution. Third, we also computed calcite and aragonite saturation states (Ω) of seawater using the pH estimates and the stratigraphically refined pCO_2 estimates. $\delta^{11}B$ data are derived from multiple species because no single species spans the entire Peniche section. Although $\delta^{11}B$ values may be affected by species-specific fractionation (Penman et al., 2013), the major shift in $\delta^{11}B$ from ~13.75‰ to ~12.5‰ within the Polymorphum Zone is recorded by the rhynchonellid *Nannirhynchia pygmaea*, and interspecific differences within weakly bioturbated beds are <0.5‰ (Fig. S4).

RESULTS AND DISCUSSION

The major and trace element composition (Sr/Ca ~0.4 – 2 mmol/mol, and Mn/Ca <0.46 mmol/mol; see the Supplemental Material and Fig. S1G) indicate very good preservation for the vast majority of our brachiopods. Brachiopod $\delta^{13}C$ and $\delta^{18}O$ records show trends similar to those previously reported from the Pl-To boundary and T-OAE (Figs. 1 and 2; Bailey et al., 2003; Suan et al., 2008). The $\delta^{13}C$ values define a short negative CIE of ~1.7‰ at the Pl-To boundary, followed by a broad positive excursion up to ~4‰ in the Polymorphum Zone, which is interrupted by a ~4‰ negative CIE diagnostic for the T-OAE. The $\delta^{18}O$ declines by ~1.8‰ within the Polymorphum Zone, followed by a negative trend up to –2.5‰ in the Levisoni Zone during the T-OAE, is also consistent with reports from elsewhere in Europe (Bailey et al., 2003; Suan et al., 2008) (Fig. 1). $\delta^{11}B$ remains rather invariant within the Spinatum (Emanciatum) Zone (oscillating around 14‰), with major changes occurring at the Pl-To boundary, where $\delta^{11}B$ first increases to almost 16‰ and subsequently declines to a minimum of ~12.5‰ in the upper Polymorphum Zone, just prior to the onset of the T-OAE (Fig. 1). $\delta^{11}B$ increases in the lower Levisoni Zone (by ~0.8‰), but reaches the lowest value (12.47‰) in the middle of the T-OAE, followed by a slight increase. A considerable change in seawater pH following the Pl-To boundary is evident from the $\delta^{11}B$ record alone. The most positive $\delta^{11}B$ values in the Spinatum Zone indicate higher pH, coinciding with the highest bulk $CaCO_3$ concentrations, the largest size of a dominant calcareous nannofossil (*Schizosphaerella*), and carbonate supersaturation (Fig. 2; Figs. S2 and S4). The overall $\delta^{11}B$ drop in the Polymorphum Zone coincides with $CaCO_3$ decline ($r = 0.36$, $p = 0.019$) and with *Schizosphaerella* size change ($r = 0.63$, $p = 0.02$) (Fig. 2; Fig. S2; Suan et al., 2010). Furthermore, $\Omega_{calcite}$ and $\Omega_{aragonite}$ decline to very low values in the Polymorphum and early Levisoni Zones (undersaturated or close to (Ω<1), Fig. S4). The changes in $\delta^{11}B$ closely follow the $\delta^{18}O$ record ($r = 0.75$, p <0.0001; based on three-point moving averages of the records). In contrast, the correlation between $\delta^{11}B$ and $\delta^{13}C$ is very weak ($r = 0.27$, $p = 0.07$).

The two ~3.5-m.y.-long $\delta^{11}B$-pH scenarios (1, brachiopod-specific $\delta^{11}B$ incorporation [Lécuyer et al., 2002]; or 2, inorganic $\delta^{11}B_{calcium\ carbonate}$ to $\delta^{11}B_{borate\ ion}$ relationship [Klochko et al.,

2006]) of seawater pH evolution differ in the absolute pH range, albeit only slightly, as a consequence of the individual δ^{11}B-pH calibration sensitivities. However, both display a sudden drop (~0.15) and an increase (~0.22) in pH in the late Pliensbachian (Margaritatus–Spinatum Zones) alongside a temperature rise and a negative CIE, implying that exogenic carbon-cycle perturbations probably started earlier in the Spinatum Zone (Fig. 2; Fig. S2). Seawater pH declined during the early Toarcian immediately after the Pl-To boundary and within an interval of ~600 k.y. during the Polymorphum Zone. The total negative shift in pH prior to the onset of the T-OAE is ~0.5. At the onset of the T-OAE (defined by the negative CIE), a sudden rise in pH by ~0.25 can be observed (Fig. 2; Fig. S2). Seawater pH reaches the minimum (~7.2) during the peak of the negative CIE and then slowly recovers, attaining pre-event values after the T-OAE. The overall decline in pH after the Pl-To boundary and prior to the T-OAE is marked by large fluctuations, which could suggest short episodic pulses (~10–200 k.y.) of volcanogenic CO_2 into the ocean-atmosphere system.

At the onset of the T-OAE negative CIE, our data indicate a sudden increase in pH that was maintained for a duration of ~270 k.y. The timing coincides with osmium isotope evidence (Cohen et al., 2004) of enhanced continental weathering due to intense temperature rise, which could have led to enhanced sequestration of atmospheric CO_2. Likewise, intensified organic carbon burial may have caused a short-term drawdown of CO_2 (Fig. 2; Fig. S2) (McElwain et al., 2005; Xu et al., 2017). The subsequent pH drop suggests that maximum CO_2 emission occurred at the peak of the negative CIE and/or that conditions maintaining carbon sequestration were no longer effective. pH evolution during the rebound phase of the negative CIE suggests slow reduction of CO_2 emission rates. When averaged to the subzone-scale stratigraphic resolution, the decline in seawater pH covaries negatively with the stomata-based pCO_2 (Pearson $r = -0.9$, $p = 0.04$, using first differences) that suggests an increase from ~850 ppm in the Spinatum Zone to ~1750 ppm throughout the T-OAE (McElwain et al. 2005; Steinthorsdottir and Vajda, 2015).

Our δ^{11}B-based pH record, sustained by stomatal pCO_2 estimates, supports a close temporal link between pH decline, early Toarcian carbon-cycle perturbations, the extinction event, and the calcification crisis. At Peniche, the late Pliensbachian–early Toarcian pH decline is associated with a long-term decline in $CaCO_3$ content, supporting the hypothesis that the significant setback of carbonate production reflects the rise in pCO_2 (Mattioli et al., 2009). Although the envelope for Ω predicted from stomata-based pCO_2, brachiopod-based pH, and δ^{18}O-based temperature is broad owing to the uncertainties in seawater δ^{11}B and δ^{11}B-pH calibration, modeled $\Omega_{aragonite}$ and $\Omega_{calcite}$ declined to the lowest levels during the late Polymorphum Zone and early Levisoni Zone (Fig. S4). Although a comparison of the δ^{11}B signal to the high-resolution $CaCO_3$ and *Schizosphaerella* records is complicated by disparate temporal resolutions of the data sets and by a delayed decline in pelagic production (relative to the neritic production; Suan et al. 2008), bivariate relations mentioned above indicate that the minima in the δ^{11}B-pH signal track low carbonate flux prior to and during the early phases of the T-OAE. The decrease in seawater pH during the Polymorphum Zone suggests that environmental conditions were already unfavorable prior to the T-OAE, and in spite of the short-term rebound in pH at the Polymorphum-Levisoni boundary, seawater likely remained undersaturated during the Levisoni Zone. Hence, in addition to warming and extensive anoxia, ocean acidification (i.e., suppressed pH and carbonate saturation state) was responsible for the biodiversity loss (Dera et al., 2010; García Joral et al., 2011; Caruthers et al., 2013) and the demise of lithiotid bivalve reefs and carbonate factories (Trecalli et al. 2012; Brame et al., 2019) during the Pl-To and T-OAE crises.

CONCLUSIONS

Our brachiopod δ^{11}B-pH reconstruction from the latest Pliensbachian–early Toarcian interval provides evidence of seawater pH decline as a result of elevated CO_2 emissions prior to the Pl-To boundary. Low-pH conditions may have developed already prior to the T-OAE. The early phase of the T-OAE was characterized by a short period of pH rebound most likely due to atmospheric CO_2 drawdown as a result of enhanced continental weathering and organic carbon burial. Seawater pH attained the lowest values immediately prior to and during the T-OAE, followed by a protracted recovery toward pre-event conditions. Our findings are congruent with the hypothesis that ocean acidification contributed to the large-scale retreat of pelagic carbonate producers and to the extinction of neritic carbonate platform builders during the early Toarcian.

ACKNOWLEDGMENTS

We thank Ana Kolevica for support of laboratory work at GEOMAR Helmholtz Centre for Ocean Research Kiel (Germany). The insights and comments from Donald Penman, Rowan Martindale, and an anonymous reviewer helped to strengthen the final version of the manuscript and are gratefully acknowledged. This project was funded by the European Union's Horizon 2020 research and innovation program under the Marie Skłodowska-Curie grant agreement and project BASE-LiNE Earth (643084) and by the Slovak Research and Development Agency (APVV17-0555) and the Slovak Scientific Grant Agency (VEGA 0169/19).

REFERENCES CITED

Bailey, T.R., Rosenthal, Y., McArthur, J.M., van de Schootbrugge, B., and Thirlwall, M.F., 2003, Paleoceanographic changes of the Late Pliensbachian–Early Toarcian interval: A possible link to the genesis of an Oceanic Anoxic Event: Earth and Planetary Science Letters, v. 212, p. 307–320, https://doi.org/10.1016/S0012-821X(03)00278-4.

Brame, H.M.R., Martindale, R.C., Ettinger, N.P., Debeljak, I., Vasseur, R., Lathuilière, B., Kabiri, L., and Bodin, S., 2019, Stratigraphic distribution and paleoecological significance of Early Jurassic (Pliensbachian-Toarcian) lithiotid-coral reefal deposits from the Central High Atlas of Morocco: Palaeogeography, Palaeoclimatology, Palaeoecology, v. 514, p. 813–837, https://doi.org/10.1016/j.palaeo.2018.09.001.

Brand, U., Azmy, K., Bitner, M.A., Logan, A., Zuschin, M., Came, R., and Ruggiero, E., 2013, Oxygen isotopes and $MgCO_3$ in brachiopod calcite and a new paleotemperature equation: Chemical Geology, v. 359, p. 23–31, https://doi.org/10.1016/j.chemgeo.2013.09.014.

Caruthers, A.H., Smith, P.L., and Gröcke, D.R., 2013, The Pliensbachian–Toarcian (Early Jurassic) extinction, a global multi-phased event: Palaeogeography, Palaeoclimatology, Palaeoecology, v. 386, p. 104–118, https://doi.org/10.1016/j.palaeo.2013.05.010.

Cohen, A.S., Coe, A.L., Harding, S.M., and Schwark, L., 2004, Osmium isotope evidence for the regulation of atmospheric CO_2 by continental weathering: Geology, v. 32, p. 157–160, https://doi.org/10.1130/G20158.1.

Comas-Rengifo, M.J., Duarte, L.V., Felix, F.F., Joral, F.G., Goy, A., and Rocha, R.B., 2015, Latest Pliensbachian–Early Toarcian brachiopod assemblages from the Peniche section (Portugal) and their correlation: Episodes, v. 38, p. 2–8, https://doi.org/10.18814/epiiugs/2015/v38i1/001.

Dera, G., Neige, P., Dommergues, J.-L., Fara, E., Laffont, R., and Pellenard, P., 2010, High-resolution dynamics of Early Jurassic marine extinctions: The case of Pliensbachian–Toarcian ammonites (Cephalopoda): Journal of the Geological Society, v. 167, p. 21–33, https://doi.org/10.1144/0016-76492009-068.

Duarte, L.V., 2007, Lithostratigraphy, sequence stratigraphy and depositional setting of the Pliensbachian and Toarcian series in the Lusitanian Basin, Portugal, *in* Rocha, R.B., ed., The Peniche Section (Portugal): Contributions to the Definition of the Toarcian GSSP: Lisbon, Portugal, International Subcommission on Jurassic Stratigraphy, p. 17–23.

Duarte, L.V., et al., 2018, The Toarcian Oceanic Anoxic Event at Peniche: An exercise in integrated stratigraphy—Stop 1.3, *in* Duarte, L.V., and Silva, R.L., eds., 2nd International Workshop on the Toarcian Oceanic Anoxic Event, Field Trip Guidebook: The Toarcian Oceanic Anoxic Event in the Western Iberian Margin and Its Context within the Lower Jurassic Evolution of the Lusitanian Basin: Coimbra, Portugal, University of Coimbra, p. 33–54.

García Joral, F., Gómez, J.J., and Goy, A., 2011, Mass extinction and recovery of the Early Toarcian (Early Jurassic) brachiopods linked to climate change in northern and central Spain: Palaeogeography, Palaeoclimatology, Palaeoecology, v. 302, p. 367–380, https://doi.org/10.1016/j.palaeo.2011.01.023.

Gattuso, J.-P., 2019, *seacarb*: Seawater Carbonate Chemistry (R package; version 3.2.12): https://CRAN.R-project.org/package=seacarb.

Gutjahr, M., Ridgwell, A., Sexton, P.F., Anagnostou, E., Pearson, P.N., Pälike, H., Norris, R.D.,

Thomas, E., and Foster, G.L., 2017, Very large release of mostly volcanic carbon during the Palaeocene–Eocene Thermal Maximum: Nature, v. 548, p. 573–577, https://doi.org/10.1038/nature23646.

Hesselbo, S.P., Gröcke, D.R., Jenkyns, H.C., Bjerrum, C.J., Farrimond, P., Bell, H.S.M., and Green, O.R., 2000, Massive dissociation of gas hydrate during a Jurassic oceanic anoxic event: Nature, v. 406, p. 392–395, https://doi.org/10.1038/35019044.

Hesselbo, S.P., Jenkyns, H.C., Duarte, L.V., and Oliveira, L.C., 2007, Carbon-isotope record of the Early Jurassic (Toarcian) Oceanic Anoxic Event from fossil wood and marine carbonate (Lusitanian Basin, Portugal): Earth and Planetary Science Letters, v. 253, p. 455–470, https://doi.org/10.1016/j.epsl.2006.11.009.

Ikeda, M., and Hori, R.S., 2014, Effects of Karoo-Ferrar volcanism and astronomical cycles on the Toarcian oceanic anoxic events (Early Jurassic): Palaeogeography, Palaeoclimatology, Palaeoecology, v. 410, p. 134–142, https://doi.org/10.1016/j.palaeo.2014.05.026.

Jenkyns, H.C., 1988, The early Toarcian (Jurassic) anoxic event: Stratigraphic, sedimentary, and geochemical evidence: American Journal of Science, v. 288, p. 101–151, https://doi.org/10.2475/ajs.288.2.101.

Jurikova, H., et al., 2019, Boron isotope systematics of cultured brachiopods: Response to acidification, vital effects and implications for palaeo-pH reconstruction: Geochimica et Cosmochimica Acta, v. 248, p. 370–386, https://doi.org/10.1016/j.gca.2019.01.015.

Klochko, K., Kaufman, A.J., Yao, W., Byrne, R.H., and Tossell, J.A., 2006, Experimental measurement of boron isotope fractionation in seawater: Earth and Planetary Science Letters, v. 248, p. 276–285, https://doi.org/10.1016/j.epsl.2006.05.034.

Krabbenhöft, A., Fietzke, J., Eisenhauer, A., Liebetrau, V., Böhm, F., and Vollstaedt, H., 2009, Determination of radiogenic and stable strontium isotope ratios ($^{87}Sr/^{86}Sr$; $\delta^{88/86}$ Sr) by thermal ionization mass spectrometry applying an $^{87}Sr/^{84}Sr$ double spike: Journal of Analytical Atomic Spectrometry, v. 24, p. 1267–1271, https://doi.org/10.1039/b906292k.

Lécuyer, C., Grandjean, P., Reynard, B., Albarède, F., and Telouk, P., 2002, $^{11}B/^{10}B$ analysis of geological materials by ICP-MS Plasma 54: Application to the boron fractionation between brachiopod calcite and seawater: Chemical Geology, v. 186, p. 45–55, https://doi.org/10.1016/S0009-2541(01)00425-9.

Littler, K., Hesselbo, S.P., and Jenkyns, H.C., 2010, A carbon-isotope perturbation at the Pliensbachian–Toarcian boundary: Evidence from the Lias Group, NE England: Geological Magazine, v. 147, p. 181–192, https://doi.org/10.1017/S0016756809990458.

Mattioli, E., Pittet, B., Petitpierre, L., and Mailliot, S., 2009, Dramatic decrease of pelagic carbonate production by nannoplankton across the Early Toarcian anoxic event (T-OAE): Global and Planetary Change, v. 65, p. 134–145, https://doi.org/10.1016/j.gloplacha.2008.10.018.

McElwain, J.C., Wade-Murphy, J., and Hesselbo, S.P., 2005, Changes in carbon dioxide during an oceanic anoxic event linked to intrusion into Gondwana coals: Nature, v. 435, p. 479–482, https://doi.org/10.1038/nature03618.

Müller, T., et al., 2017, New multiproxy record of the Jenkyns Event (also known as the Toarcian Oceanic Anoxic Event) from the Mecsek Mountains (Hungary): Differences, duration and drivers: Sedimentology, v. 64, p. 66–86, https://doi.org/10.1111/sed.12332.

Penman, D.E., Hönisch, B., Rasbury, E.T., Hemming, N.G., and Spero, H.J., 2013, Boron, carbon, and oxygen isotopic composition of brachiopod shells: Intra-shell variability, controls, and potential as a paleo-pH recorder: Chemical Geology, v. 340, p. 32–39, https://doi.org/10.1016/j.chemgeo.2012.11.016.

Percival, L.M.E., Witt, M.L.I., Mather, T.A., Hermoso, M., Jenkyns, H.C., Hesselbo, S.P., Al-Suwaidi, A.H., Storm, M.S., Xu, W., and Ruhl, M., 2015, Globally enhanced mercury deposition during the end-Pliensbachian extinction and Toarcian OAE: A link to the Karoo-Ferrar Large Igneous Province: Earth and Planetary Science Letters, v. 428, p. 267–280, https://doi.org/10.1016/j.epsl.2015.06.064.

Ridgwell, A., 2005, A Mid Mesozoic Revolution in the regulation of ocean chemistry: Marine Geology, v. 217, p. 339–357, https://doi.org/10.1016/j.margeo.2004.10.036.

Rocha, R.B., et al., 2016, Base of the Toarcian Stage of the Lower Jurassic defined by the Global Boundary Stratotype Section and Point (GSSP) at the Peniche section (Portugal): Episodes, v. 39, p. 460–481, https://doi.org/10.18814/epiiugs/2016/v39i3/99741.

Ruebsam, W., Mayer, B., and Schwark, L., 2019, Cryosphere carbon dynamics control early Toarcian global warming and sea level evolution: Global and Planetary Change, v. 172, p. 440–453, https://doi.org/10.1016/j.gloplacha.2018.11.003.

Steinthorsdottir, M., and Vajda, V., 2015, Early Jurassic (late Pliensbachian) CO_2 concentrations based on stomatal analysis of fossil conifer leaves from eastern Australia: Gondwana Research, v. 27, p. 932–939, https://doi.org/10.1016/j.gr.2013.08.021.

Suan, G., Mattioli, E., Pittet, B., Mailliot, S., and Lécuyer, C., 2008, Evidence for major environmental perturbation prior to and during the Toarcian (Early Jurassic) oceanic anoxic event from the Lusitanian Basin, Portugal: Paleoceanography, v. 23, PA1202, https://doi.org/10.1029/2007PA001459.

Suan, G., Mattioli, E., Pittet, B., Lécuyer, C., Suchéras-Marx, B., Duarte, L.V., Philippe, M., Reggiani, L., and Martineau, F., 2010, Secular environmental precursors to Early Toarcian (Jurassic) extreme climate changes: Earth and Planetary Science Letters, v. 290, p. 448–458, https://doi.org/10.1016/j.epsl.2009.12.047.

Them, T.R., II, Gill, B.C., Caruthers, A.H., Gröcke, D.R., Tulsky, E.T., Martindale, R.C., Poulton, T.P., and Smith, P.L., 2017, High-resolution carbon isotope records of the Toarcian Oceanic Anoxic Event (Early Jurassic) from North America and implications for the global drivers of the Toarcian carbon cycle: Earth and Planetary Science Letters, v. 459, p. 118–126, https://doi.org/10.1016/j.epsl.2016.11.021.

Trecalli, A., Spangenberg, J., Adatte, T., Föllmi, K.B., and Parente, M., 2012, Carbonate platform evidence of ocean acidification at the onset of the early Toarcian oceanic anoxic event: Earth and Planetary Science Letters, v. 357, p. 214–225, https://doi.org/10.1016/j.epsl.2012.09.043.

Xu, W., et al., 2017, Carbon sequestration in an expanded lake system during the Toarcian oceanic anoxic event: Nature Geoscience, v. 10, p. 129–134, https://doi.org/10.1038/ngeo2871.

Printed in USA